Available online at www.sciencedirect.com
ScienceDirect
IFAC PapersOnLine 54-20 (2021) 84–89

Disturbance Attenuation Through Real-Time Optimization of PD Gains for a Two-Link Robot ⋆

Alexander Bertino * **Hashem Ashrafiuon** ** **Peiman Naseradinmousavi** ***

* *Research Assistant, Dynamic Systems and Control Laboratory, Department of Mechanical Engineering, San Diego State University, San Diego, California 92115, USA (e-mail: abertino6245@sdsu.edu)*

** *Department of Mechanical Engineering, Villanova University, Villanova, PA 19085, USA (e-mail: hashem.ashrafiuon@villanova.edu)*

*** *Dynamic Systems and Control Laboratory, Department of Mechanical Engineering, San Diego State University, San Diego, California 92115, USA (e-mail: pnaseradinmousavi@sdsu.edu)*

Abstract: We present disturbance attenuation through PD gains optimization using real-time extremum seeking. The real-time gain optimization for a two-link robot as a case study, in particular for when we deal with a challenging five time scales problem, would provide a firm foundation to build energy-efficient multidisciplinary infrastructures from wave energy convertors (WECs) to wind turbines subject to time-varying disturbances. To the best of authors' knowledge, this is the first effort for the online learning of PD gains through the minimization of a cost function, by changing the robot's parameters to observe the attenuation of a set of harmonic disturbances while keeping the robot at the upright position. We also reveal the sensitivity of the gains' learning profiles to small changes of the disturbance and natural frequencies.

Keywords: Robotics, Control, Optimization, Disturbance Attenuation.

1. INTRODUCTION

Large-scale systems have numerous design and control parameters, which need to be optimized in order to achieve energy-efficient operation. The disturbances, either periodic or aperiodic, add to the complexity of the multivariable optimization problem, which becomes highly sensitive to the proper selection of those parameters. These factors, among others, make the offline optimization problem challenging even in the absence of disturbances. Therefore, tackling real-time optimization of any controller's gains, in the presence of disturbances, is a necessity either for small- or large-scale systems, leading us to efficiently learn optimal gains while yielding desirable responses.

The disturbance attenuation for linear systems has received considerable attention by researchers. Nguyen and Jabbari (1999) proposed a new design technique to improve disturbance attenuation for systems with input saturation. In another effort, Wang et al. (2017) developed variety of methods for attenuating or rejecting disturbances in linear systems. Nguyen and Jabbari (2000) studied output feedback controllers for disturbance attenuation of linear systems with constraints on inputs. Masuda (2012) investigated offline PID controller tuning based on disturbance attenuation through Fictitious Reference Iterative Tuning (FRIT), using one-shot experimental data due to a load change disturbance. Wei et al. (2019) addressed the problem of disturbance attenuation and rejection for a class of switched nonlinear systems subject to input and sensor saturations, in which exosystem generated disturbances and H_2-norm bounded disturbances were considered. Xiang et al. (2018) studied robust exponential stability and disturbance attenuation for discrete-time switched systems under arbitrary switching. Choi and Kwak (2001) proposed a model based disturbance attenuator (MBDA) with the conventional PD controller for robot manipulators, but not for the real-time optimization of the controller's gains.

Extremum seeking (ES), as a highly computationally efficient optimization approach, has been broadly leveraged in both linear and nonlinear systems with unknown dynamics Ariyur and Krstić (2003); Binetti et al. (2003); Cochran et al. (2009a,b); Ghaffari et al. (2014); Krstić (2000); Krstić and Wang (2000); Wang et al. (2000). The first effort for multivariable extremum seeking of general time-varying parameters was reported by Ariyur and Krstić (2002), with their other works in Ghaffari et al. (2012); Zhang et al. (2011a,b). Wang and Krstic (2000) reduced the size of a limit cycle to a minimum leveraging a novel analysis and a nontrivial sequence of steps involving averaging and singular perturbation methods. Yu et al. (2020) utilized extremum seeking to develop boundary control for freeway traffic with a downstream bottleneck. Pessoa et al.

⋆ This article is based upon work supported by the National Science Foundation under Award #1823951. The views and opinions of authors expressed herein do not necessarily state or reflect those of the United States Government or any agency thereof.

10.1016/j.ifacol.2021.11.157

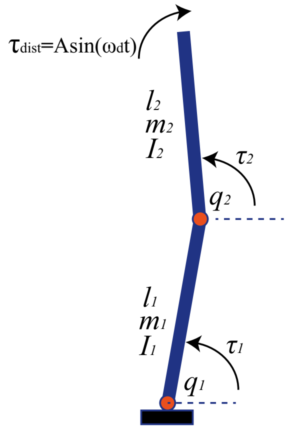

Fig. 1. The 2-DOF robot subject to a harmonic disturbance.

(2019) addressed the optimal control of carbon and nitrogen removal, using extremum seeking, from wastewaters in the presence of inhibition by substrates and products by Anaerobic Digestion Model n°1. Killingsworth and Krstic (2006) used offline extremum seeking to tune PID controllers by minimizing a cost function that characterizes the desired behavior of the closed-loop system. We previously formulated (Bagheri et al. (2018a,b)) a non-autonomous and offline joint-space trajectory optimization for one of the arms of a 7-DOF Baxter manipulator, using the state of the art discrete-time extremum seeking to be compared with the global genetic algorithm (GA). We carried out experimental work to validate the nonlinear analytical approach examining both the actual (inefficient) and optimal trajectories.

After a brief mathematical representation of a 2-DOF robot manipulator being controlled here, we set up the real-time extremum seeking to learn PD gains to attenuate the effect of harmonic disturbances, through dealing with a five time scales optimization problem. We examine different frequencies for the disturbance to reveal the high sensitivity of PD gains' learning profiles. Through simulation results, we disclose the capability of extremum seeking in the attenuation of disturbances while keeping the robot at the upright position.

2. MATHEMATICAL MODELING

We utilize a planar 2-DOF manipulator to be held at the upright position, subject to a set of harmonic disturbances with different frequencies. The robot model is shown in Fig. 1 with the following ordinary differential equations of motion (Bagheri et al. (2021, 2019); Bertino et al. (2021)) derived through the Euler-Lagrange equation:

$$M(q)\ddot{q} + C(q,\dot{q})\dot{q} + \phi(q) = \tau + \tau_{\text{dist}} \tag{1}$$

where, q, $\dot{q}$, and $\ddot{q} \in \mathbb{R}^2$ are rotation angles, angular velocities, and angular accelerations of the joints, respectively, $\tau \in \mathbb{R}^2$ indicates the vector of joints' driving torques to be optimized, and $\tau_{\text{dist}} \in \mathbb{R}^1$ stands for the harmonic disturbance acting on the top link; $\tau_{\text{dist}} = A\sin(\omega_d t)$ with A and ω_d as the amplitude and frequency of disturbance, respectively. Also, $M(q) \in \mathbb{R}^{2\times 2}$, $C(q,\dot{q}) \in \mathbb{R}^{2\times 2}$, and $\phi(q) \in \mathbb{R}^2$ are the mass, Coriolis, and gravitational matrices, respectively, which are functions of links' masses m_1, m_2, lengths l_1, l_2, and mass moments of inertia I_1, I_2.

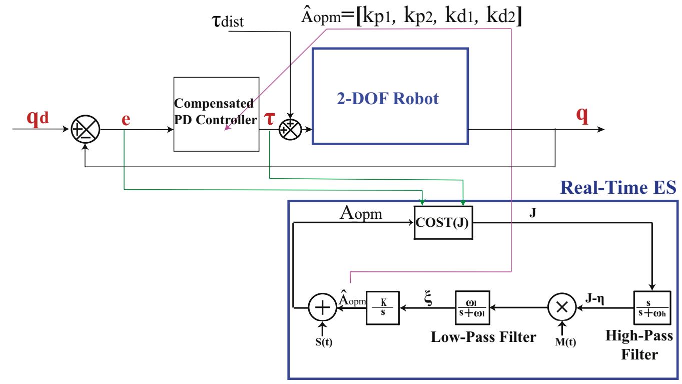

Fig. 2. The real-time extremum seeking optimizing PD gains to attenuate the harmonic disturbances.

We define the vector of error signals, $\mathbf{e} \in \mathbb{R}^2$, and its time derivative, $\dot{\mathbf{e}} \in \mathbb{R}^2$, as:

$$\mathbf{e} = q_{\text{des}} - q \tag{2}$$

$$\dot{\mathbf{e}} = \dot{q}_{\text{des}} - \dot{q} \tag{3}$$

where the desired trajectories and their first and second time derivatives, q_{des}, $\dot{q}_{\text{des}}$, $\ddot{q}_{\text{des}} \in \mathbb{R}^2$, exist and are bounded for $t \geq 0$. We employ a PD controller with gravity compensation to drive the robot as follows:

$$\tau = M(q)\left(\ddot{q}_{\text{des}} + \hat{\mathbf{k}}_p\mathbf{e} + \hat{\mathbf{k}}_D\dot{\mathbf{e}}\right) + C(q,\dot{q})\dot{q} + \phi(q) \tag{4}$$

$$\hat{\mathbf{k}}_p = \begin{bmatrix} \hat{k}_{p1} & 0 \\ 0 & \hat{k}_{p2} \end{bmatrix} \tag{5}$$

$$\hat{\mathbf{k}}_D = \begin{bmatrix} \hat{k}_{d1} & 0 \\ 0 & \hat{k}_{d2} \end{bmatrix} \tag{6}$$

where $\hat{\mathbf{k}}_p$ and $\hat{\mathbf{k}}_D$ are positive definite matrices of proportional and derivative gains to be learned in real-time using extremum seeking to attenuate the disturbances.

3. FIVE TIME SCALES OPTIMIZATION THROUGH MULTIVARIABLE REAL-TIME EXTREMUM SEEKING

The optimization is challenging in the sense that it is a five time scales problem. Briefly discussing, the disturbance has the fastest dynamics while the links (their natural frequencies ω_n's) have fast dynamics. The cost function J, to be defined in the sequel, has a medium dynamics meaning that T_J, the moving window for integration, is large relative to the natural period of oscillations of links, and small relative to the periods of the extremum seeking (ES) perturbation. The ES perturbation has a slow dynamics whereas the slowest ones belong to the learned PD gains. Dealing with such a five time scales problem leads us to carefully select the ES parameters to not only guarantee the convergence of PD gains' estimates, but also to yield a computationally efficient procedure. In summary we have:

$$T_{\text{dist}} < T_{\omega_n} < T_J < T_{\text{pert}} < T_{\text{PD}} \tag{7}$$

We define the cost function to be minimized in real time as follows:

$$J = \frac{1}{2}\int_{t-T_J}^{t}\left(\tau^T\left(\hat{\mathbf{k}}_p, \hat{\mathbf{k}}_D\right) R\tau\left(\hat{\mathbf{k}}_p, \hat{\mathbf{k}}_D\right) + \mathbf{e}^T\gamma\mathbf{e}\right)dt \quad (8)$$

where, t indicates the operation time, and γ, $R \in \mathbb{R}^{2\times 2}$ are positive definite matrices. The block diagram of Fig. 2 illustrates the real-time learning of PD gains using extremum seeking to be implemented in (4) and (8). We govern the ES to optimize the gains $A_{\text{opm}} = [k_{p1}, k_{p2}, k_{d1}, k_{d2}]^T \in \mathbb{R}^4$. Referring to the error dynamics (2) and the controller (4), the objective is to feasibly formulate the ES scheme to minimize the cost function (8) without prior knowledge of the local minimum. Noting $\hat{A}_{\text{opm}}$ as the current estimate of A_{opm}, we utilize the following equations:

$$\dot{\hat{A}}_{\text{opm}}(t) = K\zeta(t) \quad (9)$$

$$\dot{\zeta}(t) = -\omega_l\zeta(t) + \omega_l\left(J - \eta\right)M(t) \quad (10)$$

$$\dot{\eta}(t) = \omega_h\left(J - \eta\right) \quad (11)$$

$$A_{\text{opm}}(t) = \hat{A}_{\text{opm}}(t) + S(t) \quad (12)$$

In (9-12), $K \in \mathbb{R}^{4\times 4}$ is a positive definite matrix, $\zeta \in \mathbb{R}^4$, and η is a scalar. Note that the high- and low-pass filters with frequencies ω_h and ω_l yield better performing cost function and remove any DC gain, respectively. The perturbation signals $M(t)$ and $S(t)$ are calculated by (13-14).

$$M(t) = \left[\frac{2}{a_1}\sin(\omega_1 t), \cdots, \frac{2}{a_p}\sin(\omega_p t)\right]^T \quad (13)$$

$$S(t) = \left[a_1\sin(\omega_1 t), \cdots, a_p\sin(\omega_p t)\right]^T \quad (14)$$

where $p = 4$ since A_{opm} has four components and $a_1 \cdots a_p \in \mathbb{R}$ are positive coefficients. Note that $\omega_m \neq \omega_n$ for all distinct $m, n \in \{1, \cdots, p\}$. For a practically feasible ES method, we choose ω_m, ω_h, ω_l, and K through (15-18).

$$\omega_m = \alpha\omega_m' = O(\alpha) \quad m = 1, \cdots, p \quad (15)$$

$$\omega_h = \alpha\omega_H = \alpha\epsilon\omega_H' = O(\alpha\epsilon) \quad (16)$$

$$\omega_l = \alpha\omega_L = \alpha\epsilon\omega_L' = O(\alpha\epsilon) \quad (17)$$

$$K = \alpha K' = \alpha\epsilon K'' = O(\alpha\epsilon) \quad (18)$$

In (15-18), α and ϵ are small positive constants, ω_m' is a rational number, ω_H' and ω_L' are $O(1)$ positive constants, and K'' is a diagonal matrix with $O(1)$ positive elements.

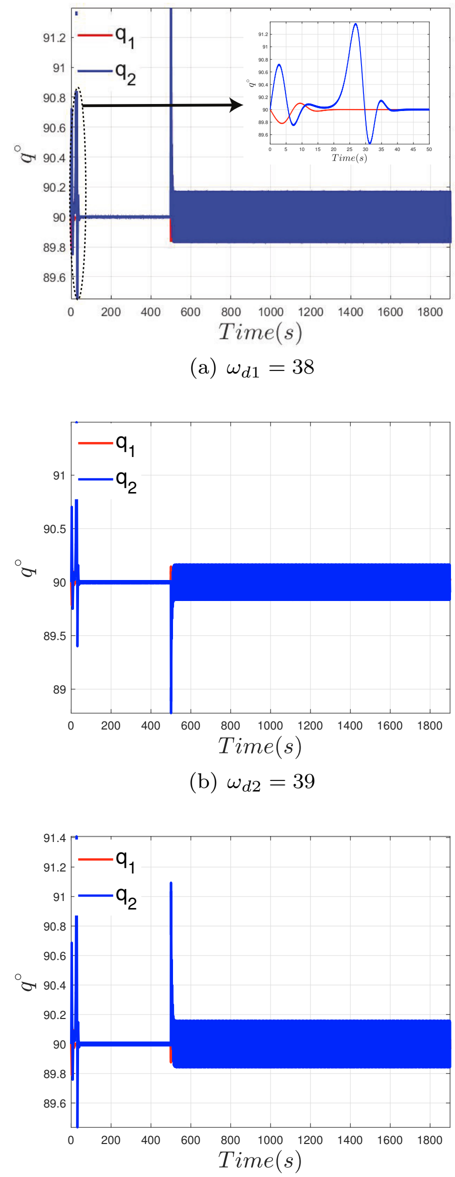

(a) $\omega_{d1} = 38$

(b) $\omega_{d2} = 39$

(c) $\omega_{d3} = 40$

Fig. 3. The controlled links' angles through the real-time ES tuning PD gains, subject to the disturbances with $\omega_{d1} = 38\left(\frac{rad}{s}\right)$ to $\omega_{d3} = 40\left(\frac{rad}{s}\right)$; $\omega_{n1} = 1.5660$, $\omega_{n2} = 1.8083$ for $0 \leq t < 500(s)$, and $\omega_{n1} = 2.5573$, $\omega_{n2} = 3.1321$ for $t \geq 500(s)$.

4. SIMULATION RESULTS

Based on the brief discussion of Section 3, we select the ES perturbation frequencies $\left(\text{in } \frac{rad}{s}\right)$ to be small relative to the natural frequencies of the links, leading us to utilize $\omega_1 = 0.14\sqrt{\frac{g}{l_1}}$, $\omega_2 = 0.13\sqrt{\frac{g}{l_2}}$, $\omega_3 = 0.12\sqrt{\frac{g}{l_1}}$, $\omega_4 = 0.11\sqrt{\frac{g}{l_2}}$, with the amplitudes of $a_1 = 0.3$, $a_2 = 0.6$, $a_3 = 0.2$, and $a_4 = 0.5$, respectively. We intentionally chose these perturbation frequencies to effectively present the sensitivity of PD gains to the changes of natural frequencies. We select the links' natural frequencies $\left(\text{in } \frac{rad}{s}\right)$ $\omega_{n1} = 1.5660$ and $\omega_{n2} = 1.8083$ for $0 \leq t < 500(s)$ with $m_1 = 2(kg)$ and $m_2 = 1.3(kg)$, and $\omega_{n1} = 2.5573$ and $\omega_{n2} = 3.1321$ for $t \geq 500(s)$ with $m_1 = 1(kg)$ and $m_2 = 0.6(kg)$ in order ro reveal the adaptive learning profiles of PD gains to attenuate the disturbances. We impose three harmonic disturbances with slightly different frequencies $\left(\text{in } \frac{rad}{s}\right)$, $\omega_{d1} = 38$, $\omega_{d2} = 39$, $\omega_{d3} = 40$, with the amplitude of $A = 0.3$. To fulfill the medium dynamics for the cost function we set $T_J = 16.3351(s)$. We choose other parameters as:

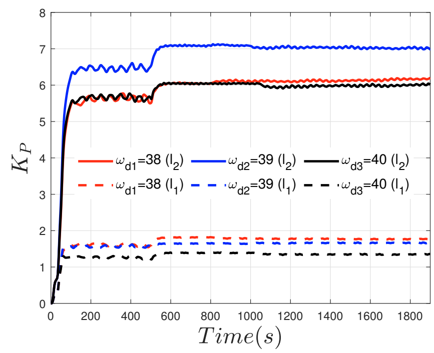

(a)

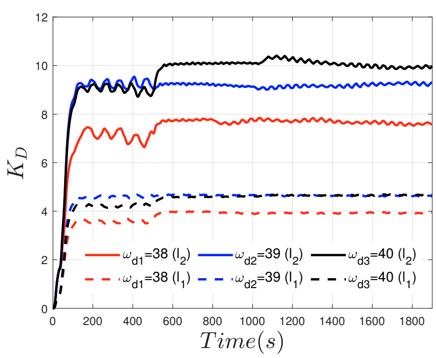

(b)

Fig. 4. The real-time learning of PD gains subject to the disturbances with $\omega_{d1} = 38 \left(\frac{rad}{s}\right)$ to $\omega_{d3} = 40 \left(\frac{rad}{s}\right)$ acting on the top link; $\omega_{n1} = 1.5660$, $\omega_{n2} = 1.8083$ for $0 \le t < 500(s)$, and $\omega_{n1} = 2.5573$, $\omega_{n2} = 3.1321$ for $t \ge 500(s)$.

$$\omega_l = 0.05 \begin{bmatrix} 1 \\ 1 \\ 1 \\ 1 \end{bmatrix}, \omega_h = 0.1, \gamma = R = I_{2\times 2}, K = 0.1 I_{4\times 4}$$

Figure 3 shows the links' angles, subject to $\omega_{d1} = 38$ to $\omega_{d3} = 40$, indicating the robot is stable around the upright position through the real-time learning of PD gains. We easily observe that the links' small deflections are relatively higher for the time interval $0 \le t < 500(s)$, with the lower natural frequencies indicating higher lengths for the links, than those of $t \ge 500(s)$ with the higher natural frequencies. Although the steady state oscillations, imposed by the algorithm, have larger amplitudes for $t \ge 500(s)$ than those of $0 \le t < 500(s)$. It is also clear that the top link, directly subject to the harmonic disturbances, slightly deflects more than the lower one, but both are stable around the upright position.

Figure 4 reveals the real-time learning of PD gains for three slightly different frequencies of the disturbance, in addition to their smooth transitions by changing the links' natural frequencies. Figure 4(a) shows the learning profiles of the proportional gain for both the top and lower links. As expected, the value of estimated proportional gain increases by the incremental disturbance frequency for the top link in comparison with the lower one. Although we may not conclude a logical correlation among the incre-

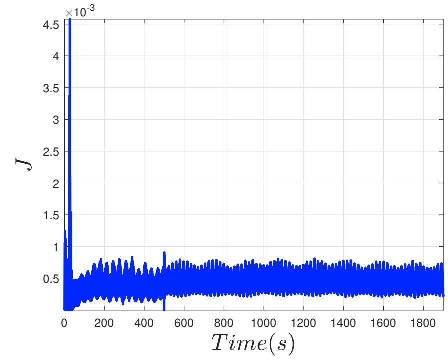

(a) $\omega_{d1} = 38$

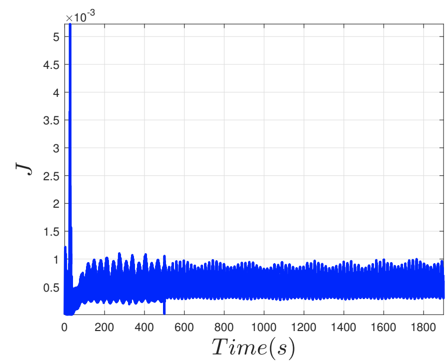

(b) $\omega_{d2} = 39$

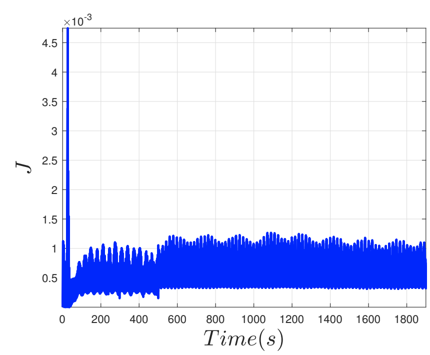

(c) $\omega_{d3} = 40$

Fig. 5. The cost function subject to the disturbances with $\omega_{d1} = 38 \left(\frac{rad}{s}\right)$ to $\omega_{d3} = 40 \left(\frac{rad}{s}\right)$.

mental values of the proportional gain for the top link whereas, with $\omega_{n2} = 3.1321$, the gain value decreases for the frequency of $\omega_{d3} = 40$ despite the cases subject to $\omega_{d1} = 38$ and $\omega_{d2} = 39$. It is interesting to observe that the proportional gain, for the lower link, decreases by increasing the disturbance frequency. Figure 4(b) presents the estimated derivative gains for the different disturbance frequencies. Despite the cases we discussed for the proportional gain, the derivative gain for the top link increases by the incremental disturbance frequency, in particular for $\omega_{n2} = 3.1321$. For the lower natural frequency of $\omega_{n2} = 1.8083$, we observe a slightly lower value of the derivative gain for $\omega_{d3} = 40$ than that of $\omega_{d2} = 39$. The lower link with $\omega_{n1} = 1.5660$ has a smaller value of the derivative gain for $\omega_{d3} = 40$ than that of $\omega_{d2} = 39$ while, for $\omega_{n1} = 2.5573$, the gains subject to $\omega_{d2} = 39$ and $\omega_{d3} = 40$ seem equal.

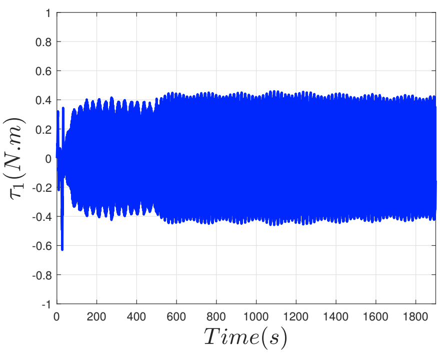

(a)

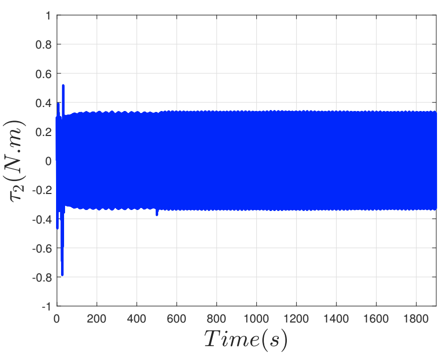

(b)

Fig. 6. The control inputs subject to the disturbance with $\omega_{d3} = 40 \left(\frac{rad}{s}\right)$.

Figure 5 presents the cost functions' profiles subject to the disturbances. We expectedly observe that the cost function settles down to a lower value for a smaller disturbance frequency. We can easily justify this behavior through the responses shown in Figs. 3 and 4. Also our intentional selection of the perturbation frequencies, as the functions of the links' natural frequencies, can be visualized through the cost function's dynamics. Shown in Fig. 6 are the control inputs, optimized through the real-time learning of PD gains, to attenuate the disturbance with $\omega_{d3} = 40$ for both the top and lower links. It is straightforward to conclude that the lower link needs more driving torque than that of the top one, and the amounts of torques decrease by reducing the disturbance frequency as shown in Fig. 7 for the case of $\omega_{d1} = 38$.

5. CONCLUSION

The principal results of this research work can be summarized as follows:

- We examined the real-time optimization of PD gains to keep the robot at the upright position, using extremum seeking, in the presence of harmonic disturbances.
- A challenging five time scales optimization problem was formulated and thoroughly discussed.
- We revealed the sensitivity of the gains' learning profiles to small changes of the disturbance and natural frequencies.

We are currently focusing our efforts on experimenting this controller using a 7-DOF Baxter robot to track a desired

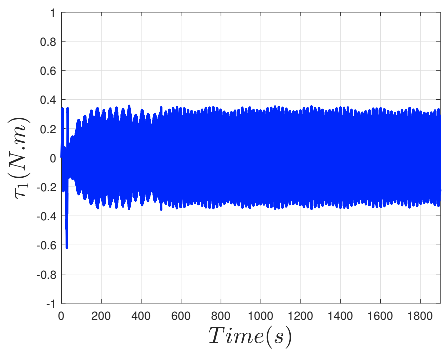

(a)

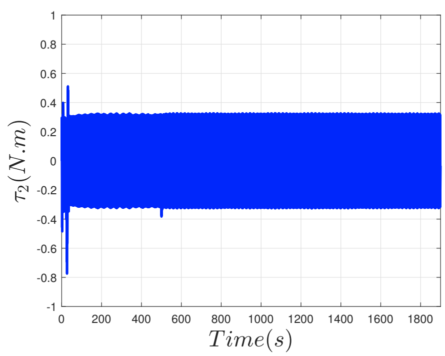

(b)

Fig. 7. The control inputs subject to the disturbance with $\omega_{d1} = 38 \left(\frac{rad}{s}\right)$.

trajectory in the presence of either periodic or aperiodic disturbances.

ACKNOWLEDGEMENTS

The authors are grateful for the valuable inputs of Professor Miroslav Krstić.

REFERENCES

Ariyur, K.B. and Krstić, M. (2002). Multivariable extremum seeking feedback: Analysis and design. In *Proc. of the Mathematical Theory of Networks and Systems*.

Ariyur, K.B. and Krstić, M. (2003). *Real-time optimization by extremum-seeking control*. John Wiley & Sons. doi:10.1002/0471669784.

Bagheri, M., Karafyllis, I., Naseradinmousavi, P., and Krstic, M. (2021). Adaptive control of a two-link robot using batch least-square identifier. *IEEE/CAA Journal of Automatica Sinica*, 8(1), 86–93.

Bagheri, M., Krstic, M., and Naseradinmousavi, P. (2018a). Joint-space trajectory optimization of a 7-DOF baxter using multivariable extremum seeking. In *2018 Annual American Control Conference (ACC)*. IEEE. doi:10.23919/acc.2018.8430959.

Bagheri, M., Krstić, M., and Naseradinmousavi, P. (2018b). Multivariable extremum seeking for joint-space trajectory optimization of a high-degrees-of-freedom robot. *Journal of Dynamic Systems, Measurement, and Control*, 140(11). doi:10.1115/1.4040752.

Bagheri, M., Naseradinmousavi, P., and Krstić, M. (2019). Feedback linearization based predictor for time delay control of a high-DOF robot manipulator. *Automatica*, 108, 108485. doi:10.1016/j.automatica.2019.06.037.

Bertino, A., Naseradinmousavi, P., and Kelkar, A. (2021). Analytical and experimental decentralized adaptive control of a high-degrees-of-freedom robot manipulator. *Journal of Dynamic Systems, Measurement, and Control*, 143(7). doi:10.1115/1.4049795.

Binetti, P., Ariyur, K.B., Krstić, M., and Bernelli, F. (2003). Formation flight optimization using extremum seeking feedback. *Journal of Guidance Control and Dynamics*, 26(1), 132–142. doi:10.2514/2.5024.

Choi, C.H. and Kwak, N. (2001). Disturbance attenuation in robot control. In *Proceedings 2001 ICRA. IEEE International Conference on Robotics and Automation (Cat. No.01CH37164)*. IEEE. doi:10.1109/robot.2001.933008.

Cochran, J., Kanso, E., Kelly, S.D., Xiong, H., and Krstić, M. (2009a). Source seeking for two nonholonomic models of fish locomotion. *IEEE Transactions on Robotics*, 25(5), 1166–1176. doi:10.1109/TRO.2009.2026500.

Cochran, J., Siranosian, A., Ghods, N., and Krstić, M. (2009b). 3-d source seeking for underactuated vehicles without position measurement. *IEEE Transactions on Robotics*, 25(1), 117–129. doi:10.1109/TRO.2008.2008742.

Ghaffari, A., Krstić, M., and Seshagiri, S. (2014). Power optimization and control in wind energy conversion systems using extremum seeking. *IEEE Transactions on Control Systems Technology*, 22(5), 1684–1695. doi:10.1109/acc.2013.6580168.

Ghaffari, A., Seshagiri, S., and Krstić, M. (2012). Power optimization for photovoltaic micro-converters using multivariable gradient-based extremum-seeking. In *American Control Conference (ACC), 2012*, 3383–3388. IEEE. doi:10.1109/ACC.2012.6314761.

Killingsworth, N.J. and Krstic, M. (2006). PID tuning using extremum seeking: online, model-free performance optimization. *IEEE Control Systems*, 26(1), 70–79. doi:10.1109/mcs.2006.1580155.

Krstić, M. (2000). Performance improvement and limitations in extremum seeking control. *Systems & Control Letters*, 39(5), 313–326. doi:10.1016/s0167-6911(99)00111-5.

Krstić, M. and Wang, H.H. (2000). Stability of extremum seeking feedback for general nonlinear dynamic systems. *Automatica*, 36(4), 595–601. doi:10.1016/S0005-1098(99)00183-1.

Masuda, S. (2012). PID controller tuning based on disturbance attenuation FRIT using one-shot experimental data due to a load change disturbance. *IFAC Proceedings Volumes*, 45(3), 92–97. doi:10.3182/20120328-3-it-3014.00016.

Nguyen, T. and Jabbari, F. (1999). Disturbance attenuation for systems with input saturation: An LMI approach. *IEEE Transactions on Automatic Control*, 44(4), 852–857. doi:10.1109/9.754833.

Nguyen, T. and Jabbari, F. (2000). Output feedback controllers for disturbance attenuation with actuator amplitude and rate saturation. *Automatica*, 36(9), 1339–1346. doi:10.1016/s0005-1098(00)00051-0.

Pessoa, R.W., Mendes, F., Oliveira, T.R., Oliveira-Esquerre, K., and Krstic, M. (2019). Numerical optimization based on generalized extremum seeking for fast methane production by a modified ADM1. *Journal of Process Control*, 84, 56–69. doi:10.1016/j.jprocont.2019.09.006.

Wang, H.H. and Krstic, M. (2000). Extremum seeking for limit cycle minimization. *IEEE Transactions on Automatic Control*, 45(12), 2432–2436. doi:10.1109/9.895589.

Wang, H.H., Yeung, S., and Krstić, M. (2000). Experimental application of extremum seeking on an axial-flow compressor. *IEEE Transactions on Control Systems Technology*, 8(2), 300–309. doi:10.1109/87.826801.

Wang, J., Yue, H., and Dimirovski, G. (2017). Disturbance attenuation in linear systems revisited. *International Journal of Control, Automation and Systems*, 15(4), 1611–1621. doi:10.1007/s12555-016-0132-5.

Wei, Y., Sun, L., Jia, S., Liu, K., and Meng, F. (2019). Disturbance attenuation and rejection for a class of switched nonlinear systems subject to input and sensor saturations. *Mathematical Problems in Engineering*, 2019, 1–13. doi:10.1155/2019/5653619.

Xiang, W., Tran, H.D., and Johnson, T.T. (2018). Robust exponential stability and disturbance attenuation for discrete-time switched systems under arbitrary switching. *IEEE Transactions on Automatic Control*, 63(5), 1450–1456. doi:10.1109/tac.2017.2748918.

Yu, H., Koga, S., Oliveira, T.R., and Krstic, M. (2020). Extremum seeking for traffic congestion control with a downstream bottleneck. *Journal of Dynamic Systems, Measurement, and Control*, 143(3). doi:10.1115/1.4048781.

Zhang, Y., Rotea, M., and Gans, N. (2011a). Sensors searching for interesting things: Extremum seeking control on entropy maps. In *Decision and Control and European Control Conference (CDC-ECC), 2011 50th IEEE Conference on*, 4985–4991. IEEE. doi:10.1109/cdc.2011.6161146.

Zhang, Y., Shen, J., Rotea, M., and Gans, N. (2011b). Robots looking for interesting things: Extremum seeking control on saliency maps. In *Intelligent Robots and Systems (IROS), 2011 IEEE/RSJ International Conference on*, 1180–1186. IEEE. doi:10.1109/iros.2011.6095014.